

Analysis of Blocking in mmWave Cellular Systems: Application to Relay Positioning

Cristian García*, Antonio Pascual-Iserte[†], *Senior Member, IEEE*, Olga Muñoz[‡],
Member, IEEE

Dept. of Signal Theory and Communications

Universitat Politècnica de Catalunya, Barcelona, Spain

Email: *cristian.garcia.ruiz@estudiant.upc.edu, [†]antonio.pascual@upc.edu,
[‡]olga.munoz@upc.edu

Abstract

Within the framework of 5G, blockage effects occurring in the mmWave band are critical. These blockages can be statistically modeled with mathematical tools such as stochastic geometry and random shape theory. In the literature, there are studies describing the effects of blockages in both isolated and multiple links for simple blocking objects. Our study considers a scenario in which there are N links and takes into account the possible correlation among them in terms of blocking by extending previous works to more general blocking objects. This paper also applies the formulation developed for the case of N links to optimize the relay positioning in mmWave cells for coverage enhancement, that is, to minimize in average the probability of blockage within the cell, which is another contribution of this work. The paper includes numerical evaluations that highlight the fact that considering independence among the blocking elements of the links is a too brief simplification and does not describe accurately the real scenario. We also show the effect of taking into account more realistic blocking objects than those considered so far in the literature and the impact of the positioning of the relays on the coverage.

Index Terms

mmWave, blockage, stochastic geometry, random shape theory, relay.

I. INTRODUCTION

A. *Background and Motivation*

Users demand day after day much faster, higher capacity and broader coverage in mobile communications. A huge number of new social applications and the growing interest for the mobile market has acted as a catalyst in this field. Existing technologies, including long term evolution (LTE), have served well for many years but, since some time ago, it has been shown that a new generation of mobile communications is needed.

There are some applications that are just taking off requiring standards that provide higher quality than previous generations of mobile communications. An example is the increasing interest in autonomous cars, that have to share information in real time with each other so as to make autonomous driving possible. Communications have to support high traffic, secure and almost instantaneous information transmission, as explained in [1]. As another example, the Internet of things (IoT) arises the need for supporting very dense networks as well.

These are just some of the many reasons why the technological community is adopting the new communications standard known as 5G [2]. In order to meet the requirements exposed above, it has been agreed that the usage of mmWave bands (that is, frequencies above 6 GHz) is needed [3]. The main reason for this is that mmWave allows larger bandwidths, which results in higher data rates, as explained in [4]. This band has been widely studied for indoor usage, such as wireless local area networks (WLANs), while it has just recently been considered for mobile cellular communications as well.

Note, however, that the use of the mmWave bands implies several important negative effects that should be taken into account. The first one is the high attenuation and penetration losses in comparison with lower frequencies used in previous standards. Another effect to consider is the bad diffraction of the electromagnetic waves [1] due to the fact that the wavelength is typically smaller than the sizes of objects in the environment. The main consequence is that any object with an electric size higher than the wavelength (which happens very frequently due to the small wavelength) will block the signal propagation, provoking blockages. In other words, in mmWave signal transmission, successful transmission requires line of sight (LOS), that is, no blockage, between the transmitter and the receiver. These effects should be considered explicitly in the network design as it has a direct impact on the coverage.

Due to the previous reasons, we need a framework to statistically model blockages and their

impact on the coverage. Also, a proper strategy to improve the coverage is needed. This is the motivation of this work. The starting point is based on [5] and [6] that use stochastic geometry [7], [8], [9] to model the number of blocking elements and their positions. In order to simplify the analysis, blockages are assumed to be uniformly distributed along space following a Poisson point process (PPP). The blocking elements (e.g. buildings) may have different shapes. Basically, three models of blocking elements are taken into account: line segments without height, rectangles without height, and line segments with height, whose sizes and orientations are modeled as random through random shape theory [10]. These papers obtain the probability of blockage for specific and isolated links. When multiple links are considered, the assumption that the blockages on each of them are independent might be inaccurate. For instance, if the angle between two links is small, it is likely that the links will have some blockages in common. This fact is shown in [11], [12] and [13], in which the correlation between the blockings of different links is considered but only for the case of line segments. In all the works referenced previously, the positions of the transmitters and receivers are non-random and known.

Authors in [14] consider the concrete case of rectangles whose lengths are Gaussian distributed. Height is incorporated using the same procedure as in [6]; however, that procedure is only valid for the case of line segments with height, but not for volumes. In [14], multiple links to several access points are considered but the correlation of the blocking among these links is not taken into account.

A way to improve coverage is through the use of relays. A network with a transmitter and a receiver at given positions and relays at random positions is addressed in [15]. For this network, the performance is analyzed without incorporating the correlation among the blockages in different user-relay links. In [16], a network is considered with one transmitter and several nodes at concrete static positions. Whenever a node is blocked, it can connect to another one that takes the role of relay. The node selected for relaying is that having the lowest probability of being blocked. In that paper, the blocking elements are modeled as a PPP with circles having given radius and without height, which avoids the need for using random shape theory.

In this paper, we make a statistical analysis of the effects of blockages in the scenario of multiple links without considering independence among them, as done in [11] and [12], but considering more general blocking object shapes. As an example of application, we make use of this analysis to optimize the positions of a set of relays in a mobile cell with the aim of minimizing the impact of blockage, that is, improving the coverage of the network.

B. Goals and Contributions

In this paper, we characterize statistically the impact of the blocking effect on the probability of having a successful transmission, that is, being in coverage. As an application, we consider a cellular system where several relays are used to improve that probability. The work studies how the optimal positions of the relays depends on the density and shapes of the blocking elements.

The number and positions of blockages are considered to be random, where such randomness is modeled through stochastic geometry, assuming PPP, and the shapes of the blocking buildings are modeled through random shape theory.

Next, we list the main contributions of this paper with respect to the works referenced previously:

- Derive the blocking element model corresponding to a rectangle with height (i.e., the model closest to a real building).
- Consider a set of N links and take into account the correlation among the blockings in these links. This is done for the most general case of blockages: rectangles with height.
- Apply the obtained formulation to the mobile cell scenario and use it to design a relay based network deployment for the most general case of blockages: rectangles with height.
- Formulate the probability of coverage in the presence of relays without assuming independence among the links of the scenario. This probability is averaged over any possible position of the user within the cell, providing a global figure of merit of the cell coverage.
- Find the optimum positions of the relays to improve the average probability of coverage (that is, to minimize the average probability of not having successful transmission), where the average is taken not only with respect to the randomness of the blockings, but also with respect to the random position of the user.
- Show that these optimum positions of the relays are highly influenced by the correlation among the blockages affecting the links within the cell.
- Validate the analytical expressions through simulations.
- Consider sensitivity parameters at the receiver, antenna gains and power losses into the expressions of successful transmission. This is extremely important since, due to signal attenuation, long links may produce unsuccessful transmission even in LOS conditions.

C. Organization

The paper is organized as follows. In Section II, we describe the effects of blockage in a single-link scenario for different models of blocking elements. In Section III, we apply the concepts obtained for every model of blocking element to a scenario with multiple links and derive the formulation of the probability of having successful transmission. In Section IV, we apply the results obtained in previous sections to the analysis of relay-based communications in terms of the probability of coverage averaged over the random user position. We also take into account parameters related to power and sensitivity as well. A comparison between simulation results and the analytical expressions derived in this work can be found in Section V. Finally, conclusions are detailed in Section VI.

D. Notation

In this paper, we make use of the following notation:

- Given a region S in \mathbb{R}^n (i.e., $S \subset \mathbb{R}^n$) we define the indicator function $\mathbb{1}_S(\mathbf{x})$, $\mathbf{x} \in \mathbb{R}^n$ as

$$\mathbb{1}_S(\mathbf{x}) := \begin{cases} 1 & \text{if } \mathbf{x} \in S \\ 0 & \text{if } \mathbf{x} \notin S. \end{cases} \quad (1)$$

In the case that $S \subset \mathbb{R}^2$, the area of region S is defined as:

$$A_S = \int \mathbb{1}_S(\mathbf{x}) d\mathbf{x}. \quad (2)$$

- $K \sim \mathcal{P}(\bar{K})$ indicates that K is a random variable (r.v.) following a Poisson distribution with mean value $\bar{K} = \mathbb{E}[K]$. $X \sim \mathcal{U}[a, b]$ indicates that X is a uniform r.v. in $[a, b]$.
- When applied to events in the calculation of probabilities, \vee stands for ‘or’ and \wedge stands for ‘and’.

II. SINGLE-LINK COMMUNICATION

In this section, we assume that there is a single-link with one transmitter and one receiver, denoted as (0) and (1) in Fig. 1, respectively, being d the distance between them. As commented previously, due to the use of mmWave bands, the transmission will be successful whenever there is LOS between (0) and (1), that is, whenever there is no object blocking the segment connecting both nodes since just a single blocking element may result into a loss of many dB in the signal level [1], [4]. In this paper, we assume that the positions of the potentially blocking elements are

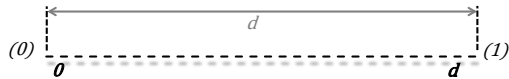


Fig. 1: Single link with one transmitter and one receiver.

random and follow a PPP, which means that the number of blocking elements in a given area is also random and follows a Poisson distribution (check [7], [8], [9], [17] for some references). Also, the shapes and the sizes of these blocking elements are modeled as r.v.'s through random shape theory [10].

A. Probability of Blockage

The fact that the positions of the blocking elements are modeled following a PPP implies that:

- the number of potentially blocking objects in a given region is a Poisson r.v.,
- the number of elements blocking a given concrete link (such as the one represented in Fig. 1), denoted by K , is a r.v. that follows a Poisson distribution with parameter $\mathbb{E}[K]$ [18].

Having non-LOS (NLOS) in a given link means having one or more blocking elements in the link. Accordingly, we will compute the probability of having blockage following a similar procedure to that used in [5], [6]. If we denote the probability of not having successful transmission because of the blocking by $\mathbb{P}(KO)$ (i.e., not being in coverage), we have:

$$\mathbb{P}(KO) = 1 - \mathbb{P}(K = 0) = 1 - e^{-\mathbb{E}[K]}. \quad (3)$$

Accordingly, the problem results into obtaining an analytic expression for $\mathbb{E}[K]$. We will present this for four different models of blocking elements detailed in subsection II-B. The formulation for the first three models (subsections II-B1, II-B2, II-B3) was already presented in [5], [6], however, in this paper we follow a different methodology to obtain those formulations that will allow us to generalize the derivation for the fourth model (subsection II-B4). Also, this novel methodology will be used to extend this analysis to the multiple-link cases and the relay-based scenario in Sections III and IV in this paper, also considering the four models.

In all cases, we assume that the spatial density of potentially blocking elements is uniform in all the space and denoted by λ [blocking elements per m^2]. In the following, we also assume that the shapes (sizes and orientations) of the blocking elements are independent among them.

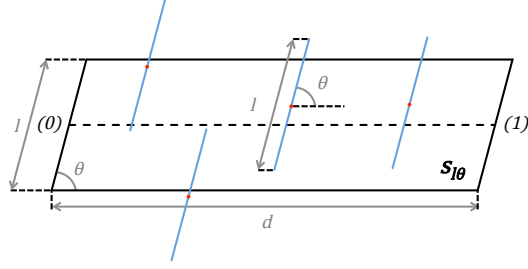


Fig. 2: Parallelogram corresponding to the line segments model.

When we talk about the positions of the blocking elements, we refer to the centers of their bases, as will be illustrated in the corresponding figures.

B. Modeling of the Blocking Elements Based on Random Shape Theory

1) *Line Segments Model*: In this model, blocking elements are considered to be line segments of random lengths L and orientations Θ drawn from the probability density functions (pdf's) $f_L(l)$ and $f_\Theta(\theta)$. Accordingly, the spatial density of blocking elements with lengths and orientations in the differential intervals $[l, l + dl]$ and $[\theta, \theta + d\theta]$, respectively, is given by $\lambda_{l\theta} = \lambda f_L(l) dl f_\Theta(\theta) d\theta$. Line segments of a given length l and an orientation θ effectively block the link connecting nodes (0) and (1) of length d if, and only if, their centers fall within the parallelogram $S_{l\theta}$ shown in Fig. 2 (see also Fig. 2 in [5]). In this case, $A_{S_{l\theta}} = |ld \sin \theta|$. Additionally, by assuming that the blocking elements can have any orientation with equal probability¹, that is, $f_\Theta(\theta) = \frac{1}{\pi}$ with $\Theta \sim \mathcal{U}[0, \pi]$, it is possible to write directly the modulus as $|ld \sin \theta| = ld \sin \theta$. Being $K_{l\theta}$ the number of line segments with length in $[l, l + dl]$ and orientation in $[\theta, \theta + d\theta]$ blocking the link, in [5] it is shown that $K_{l\theta} \sim \mathcal{P}(\overline{K_{l\theta}})$, with mean value $\overline{K_{l\theta}} = \lambda_{l\theta} A_{S_{l\theta}}$. Taking everything into account, the total number of elements K blocking the transmission is also a Poisson r.v. resulting from the aggregation of all the possible lengths and orientations with mean value

$$\mathbb{E}[K] = \int_l \int_\theta \mathbb{E}[K_{l\theta}] = \beta d, \quad (4)$$

where $\beta = \frac{2\lambda \mathbb{E}[L]}{\pi}$.

¹From now on, we will make this assumption for the sake of simplicity, unless stated otherwise.

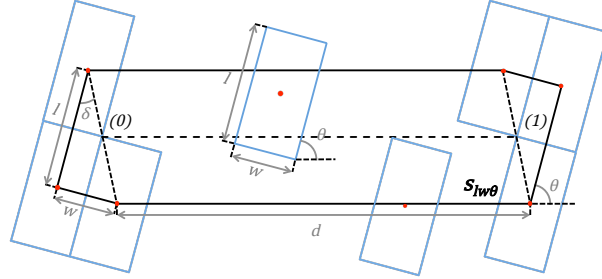


Fig. 3: Polygon corresponding to the rectangle model.

2) *Rectangles Model*: In this model, each blocking element is modeled as a rectangle with a certain length l , width w , and orientation θ drawn from the r.v.'s L , W and Θ , respectively. Accordingly, we denote by $S_{lw\theta}$ the geometric locus composed of the centers of all the possible blocking elements. For example, we have the polygon shown in Fig. 3 (see also Fig. 1 in [6]). In [6], it is shown that the number of blocking elements with lengths, widths and orientations in the differential intervals $[l, l+dl]$, $[w, w+dw]$ and $[\theta, \theta+d\theta]$, respectively, denoted by $K_{lw\theta}$, is a Poisson r.v. with mean value given by $\overline{K_{lw\theta}} = \lambda_{lw\theta} A_{S_{lw\theta}}$, where $\lambda_{lw\theta} = \lambda f_L(l) dl f_W(w) dw f_\Theta(\theta) d\theta$ and $A_{S_{lw\theta}} = d(l \sin \theta + w |\cos \theta|) + wl$.

Therefore, considering all the possible lengths, widths and orientations, in [6] it is shown that $K \sim \mathcal{P}(\beta d + p)$ with $\beta = \frac{2\lambda(\mathbb{E}[L] + \mathbb{E}[W])}{\pi}$ and $p = \lambda \mathbb{E}[L] \mathbb{E}[W]$.

3) *Line Segments with Height Model*: The next step is to incorporate height in the line segments model, which means that the base of the blocking element is a line of length l and orientation θ , as previously, but a height h is considered as well, obtaining a vertical rectangle, as illustrated in Fig. 4 (see also Fig. 2 in [6]). The values of l , θ and h are drawn from the r.v.'s L , Θ and H . In the next figures (Fig. 4, 5 and 6), the extreme points (0) and (1) of the link under analysis are considered to have also a certain height. For this reason, and just to give an example, we have placed a base station (BS) and a mobile phone in (0) and in (1) with heights H_0 and H_1 , respectively. This will help us in the understanding of the effect produced by the height of the blocking elements, which is developed in this subsection II-B3 and also in subsection II-B4.

Following Fig. 4, the line segments placed at distance y from (0) that effectively block the link are the ones whose height h is higher than the height of the link with respect to the ground at that point y .

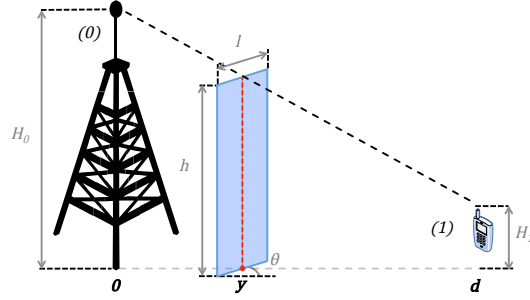


Fig. 4: Height effect on the line segments based model.

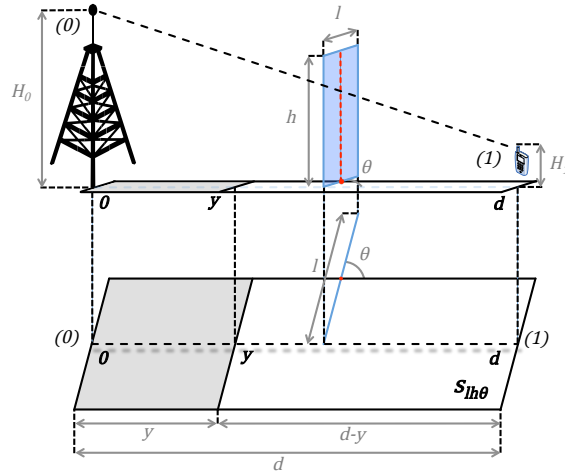


Fig. 5: Decrease of the size of the parallelogram $S_{l\theta}$ corresponding to the line segments model.

As we have stated before, K is the number of blocking elements that effectively block the considered link. K follows a Poisson distribution whose mean is obtained as follows:

$$\mathbb{E}[K] = \int_l \int_h \int_\theta \mathbb{E}[K_{lh\theta}] = \int_l \int_h \int_\theta \lambda_{lh\theta} A_{S_{lh\theta}}, \quad (5)$$

where $K_{lh\theta}$ is the number of elements blocking the link with lengths, heights and orientations in the differential intervals $[l, l + dl]$, $[h, h + dh]$ and $[\theta, \theta + d\theta]$, respectively. $K_{lh\theta}$ follows a Poisson distribution with mean value $\overline{K_{lh\theta}} = \lambda_{lh\theta} A_{S_{lh\theta}}$, where $\lambda_{lh\theta} = \lambda f_L(l) dl f_H(h) dh f_\Theta(\theta) d\theta$. What differs now from the previous cases is that the expression of $A_{S_{lh\theta}}$ changes depending on the considered h , as illustrated in Fig. 5. That figure shows the geometric locus of blocking elements of length l , height h and orientation θ . Even though this region is a parallelogram, as it happened in the line segments model (subsection II-B1), there is a difference between these models: now, the length of the base of the parallelogram is $d - y$ instead of d (which is the

length for the case of segments without height shown in subsection II-B1 and Fig. 2), therefore, it is y meters lower. By geometrical reasoning, y is calculated as:

$$y = \frac{H_0 - h}{H_0 - H_1}d \quad \Rightarrow \quad d - y = \frac{h - H_1}{H_0 - H_1}d. \quad (6)$$

In other words, the shadowed area is the region of $S_{l\theta}$ that, because of taking height into account, does not belong to the subset $S_{lh\theta}$. Finally, we can compute $A_{S_{lh\theta}}$ as:

$$A_{S_{lh\theta}} = \begin{cases} ld \sin \theta & \text{if } h > H_0 \\ \left(\frac{h - H_1}{H_0 - H_1} \right) ld \sin \theta & \text{if } H_1 \leq h \leq H_0 \\ 0 & \text{if } h < H_1. \end{cases} \quad (7)$$

By replacing $\lambda_{lh\theta}$ and (7) in (5), we obtain

$$\begin{aligned} \mathbb{E}[K] &= \int_l \int_h \int_\theta \mathbb{E}[K_{lh\theta}] \\ &= \beta d \left(\int_{H_1}^{H_0} \frac{h - H_1}{H_0 - H_1} f_H(h) dh + \int_{H_0}^{\infty} f_H(h) dh \right) \\ &= \beta d \left(1 - \frac{1}{H_0 - H_1} \int_{H_1}^{H_0} F_H(h) dh \right) \\ &= \eta \beta d, \end{aligned} \quad (8)$$

with $\beta = \frac{2\lambda\mathbb{E}[L]}{\pi}$ and $\eta = 1 - \frac{1}{H_0 - H_1} \int_{H_1}^{H_0} F_H(h) dh$, where $F_H(h)$ is the cumulative density function (cdf) of the r.v. H .

It can be concluded that the effect of adding height to the line segments model of blocking elements turns into a scaling factor η over the mean number of blocking elements that is obtained in the line segments model. This coincides with the result in Subsection III.B in [6], although a different procedure has been followed.

4) *Rectangles with Height Model:* This subsection is a novel contribution with respect to the existing state of the art since it generalizes the concept seen before by adding the effect of the height in the rectangle model of blocking elements. With this step, we can characterize the effect of 3D blockage produced by rectangular buildings with height, which is pretty close to the real scenario that should be faced in cities. For each building, it is assumed that the dimensions and orientation l , w , h and θ are drawn from the r.v.'s L , W , H and Θ , respectively.

As shown in Fig. 6, when incorporating height into the rectangle model, the effect is the same as in the line segments model: depending on the height of the blockage, the region $S_{lwh\theta}$ that contains the centers of all the blocking elements with length l , width w , height h and orientation θ gets smaller when compared to Fig. 3 in subsection II-B2, while the shape remains the same.

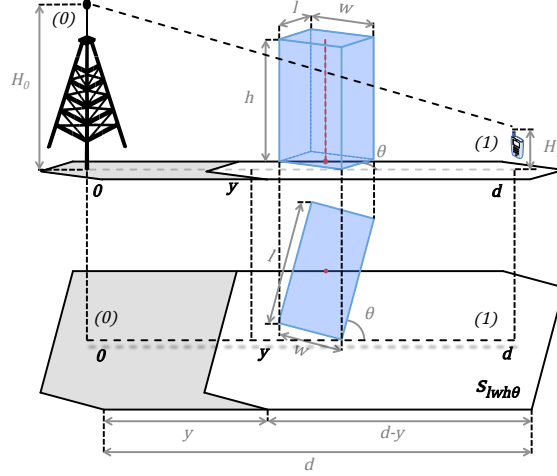


Fig. 6: Polygon corresponding to the rectangle model including the effect of the height.

$K_{lwh\theta}$ is the number of elements blocking the link with lengths, widths, heights and orientations in the differential intervals $[l, l + dl]$, $[w, w + dw]$, $[h, h + dh]$ and $[\theta, \theta + d\theta]$, respectively. It follows a Poisson distribution with mean value given by $\overline{K_{lwh\theta}} = \lambda_{lwh\theta} A_{S_{lwh\theta}}$ where $\lambda_{lwh\theta} = \lambda f_L(l) dl f_W(w) dw f_H(h) dh f_\Theta(\theta) d\theta$ and

$$A_{S_{lwh\theta}} = \begin{cases} d(l \sin \theta + w |\cos \theta|) + wl & \text{if } h > H_0 \\ \left(\frac{h-H_1}{H_0-H_1}\right) d(l \sin \theta + w |\cos \theta|) + wl & \text{if } H_1 \leq h \leq H_0 \\ 0 & \text{if } h < H_1. \end{cases} \quad (9)$$

The mean value of K , which is the total number of elements effectively blocking the transmission through the considered link that follows a Poisson distribution, is:

$$\begin{aligned} \mathbb{E}[K] &= \int_l \int_w \int_h \int_\theta \mathbb{E}[K_{lwh\theta}] \\ &= \beta d \left(\int_{H_1}^{H_0} \frac{h-H_1}{H_0-H_1} f_H(h) dh + \int_{H_0}^{\infty} f_H(h) dh \right) + p \int_{H_1}^{\infty} f_H(h) dh \\ &= \beta d \left(1 - \frac{1}{H_0-H_1} \int_{H_1}^{H_0} F_H(h) dh \right) + p(1 - F_H(H_1)) \\ &= \eta \beta d + \mu p, \end{aligned} \quad (10)$$

with $\beta = \frac{2\lambda(\mathbb{E}[L]+\mathbb{E}[W])}{\pi}$, $p = \lambda \mathbb{E}[L] \mathbb{E}[W]$, $\eta = 1 - \frac{1}{H_0-H_1} \int_{H_1}^{H_0} F_H(h) dh$ and $\mu = 1 - F_H(H_1)$. As already mentioned, the previous expression is a novelty with respect to the state of the art. Note that the previous expression is more accurate than eq. (4) derived in [14]. In [14], it is considered that a 3D building does not block the link if the height at the center of the building

does not block the vision, whereas in expression (10) it is considered the fact that LOS requires additionally that the faces of the 3D building do not block the vision.

Particularizing, if we assume $H \sim \mathcal{U}[0, H_{max}]$, the parameters η and μ can be easily derived, leading us to the expressions (11) and (12):

$$\eta = \begin{cases} 1 - \frac{H_0 + H_1}{2H_{max}} & \text{if } 0 \leq H_1 \leq H_0 \leq H_{max} \\ 1 - \frac{1}{H_0 - H_1} \left(\frac{H_{max}^2 - H_1^2}{2H_{max}} + H_0 - H_{max} \right) & \text{if } 0 \leq H_1 \leq H_{max} \leq H_0 \\ 0 & \text{if } 0 \leq H_{max} \leq H_1 \leq H_0 \end{cases} \quad (11)$$

$$\mu = \begin{cases} \frac{H_{max} - H_1}{H_{max}} & \text{if } 0 \leq H_1 \leq H_{max} \\ 0 & \text{if } 0 \leq H_{max} \leq H_1 \end{cases} \quad (12)$$

It is important to emphasize that considering generic pdf's for the lengths, widths, orientations and heights of the blocking elements allows to consider, as particular cases, several typical situations. For example, in urban environments, buildings may have deterministic widths or orientations. In such cases, the corresponding r.v.'s would just be deterministic and, consequently, the corresponding integrations can be calculated in closed-form (remember that for a deterministic variable x taking value x_0 , the pdf is given by $\delta(x - x_0)$ and $\int g(x)\delta(x - x_0)dx = g(x_0)$).

As an illustrative example, let us assume that all buildings have the same given widths, lengths, heights and orientations denoted by w_0 , l_0 , h_b (with $H_1 < h_b < H_0$) and $\theta = 0$, respectively. Then, the following simple closed-form expression is obtained:

$$\mathbb{E}[K] = \lambda w_0 \left(\frac{h_b - H_1}{H_0 - H_1} d + l_0 \right).$$

Following the same procedure, other simplifications could be obtained by considering other cases of deterministic values for some of the parameters of the blocking objects.

III. MULTIPLE-LINK COMMUNICATION

In the previous section, we have seen several ways of characterizing the effect of blockage in isolated links. Particularly, we have gone through four different models for the blocking elements and reached a general one consisting in the rectangles with height, which is the most realistic model for buildings in urban scenarios.

This section generalizes the previous one by considering multiple links. An example can be shown for the case of 2 and N links in Fig. 7a and 7b, respectively.

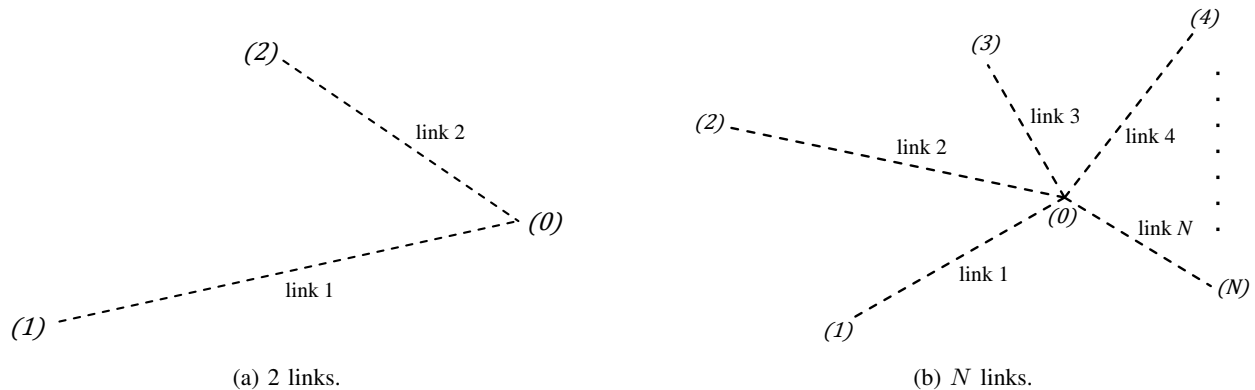


Fig. 7: Multiple-link communication scenario.

Let K_i and K_j denote the number of blocking elements that effectively block the links i and j , respectively, while $K_{i,j}$ is the number of blocking elements that obstruct link i or link j . In general, when \mathcal{A} is a set of links, $K_{\mathcal{A}}$ denotes the number of blocking elements that effectively block at least one of the links in that set.

In the following, $\mathbb{P}(OK_i)$ and $\mathbb{P}(KO_i)$ denote the probabilities of having and not having successful transmission through link i , respectively. On the other hand, $\mathbb{P}(\text{any}OK)$ is the probability of having successful transmission through, at least, one of the N links, while $\mathbb{P}(\text{all}KO)$ is the probability of not having successful transmission through any link.

The simplistic assumption that the blockings on each link are independent might not always hold. For instance, if two links are close in terms of the azimuth from a node's perspective, the probability of existing an element blocking both links at the same time is high. On the other hand, the hypothesis of independence does not hold when the lengths of links are small in terms of the length of the blocking elements. This will be evaluated in the simulations section.

This section generalizes previous works such as [5] and [6] that did not consider correlation among links, and [11] and [12] that took into account the correlation for the case of blockages modeled as segments without height. The derivations presented in this section are valid for the most general case of rectangles with height. In order to obtain the corresponding expressions, we will first consider only 2 links. Then, we will analyze the 3 links situation and, finally, generalize the expression to N links.

A. Two Links

The calculation of $\mathbb{P}(\text{all}KO)$ and $\mathbb{P}(\text{any}OK)$ can be expressed as follows:

$$\begin{aligned}\mathbb{P}(\text{all}KO) &= 1 - \mathbb{P}(\text{any}OK) = 1 - \mathbb{P}(OK_1 \vee OK_2) \\ &= 1 - \mathbb{P}(OK_1) - \mathbb{P}(OK_2) + \mathbb{P}(OK_1 \wedge OK_2).\end{aligned}\quad (13)$$

While we have that $\mathbb{P}(OK_1) = e^{-\mathbb{E}[K_1]}$ and $\mathbb{P}(OK_2) = e^{-\mathbb{E}[K_2]}$, $\mathbb{P}(OK_1 \wedge OK_2)$ remains unknown. This term is the probability that there are not blockages neither in link 1 nor in link 2. To be general, we take the rectangles with height model of blocking elements. Let us first consider a specific length l , width w , height h and orientation θ of the blocking elements. Accordingly, both links will be in LOS when no centers of the blocking elements fall within $S_{1_{lwh\theta}} \cup S_{2_{lwh\theta}}$. Generalizing the result to any length, width, height and orientation and being $K_{1,2}$ the number of blockages that effectively block at least one of the 2 links, we can state that $\mathbb{P}(OK_1 \wedge OK_2) = \mathbb{P}(K_{1,2} = 0) = e^{-\mathbb{E}[K_{1,2}]}$. Replacing it in (13), we obtain:

$$\mathbb{P}(\text{all}KO) = 1 - \mathbb{P}(\text{any}OK) = 1 - e^{-\mathbb{E}[K_1]} - e^{-\mathbb{E}[K_2]} + e^{-\mathbb{E}[K_{1,2}]}. \quad (14)$$

In order to make a quick comparison, we now present the probability of blockage assuming that blockages in every link are independent:

$$\begin{aligned}\mathbb{P}(\text{all}KO) &= \mathbb{P}(KO_1)\mathbb{P}(KO_2) = (1 - e^{-\mathbb{E}[K_1]}) (1 - e^{-\mathbb{E}[K_2]}) \\ &= 1 - e^{-\mathbb{E}[K_1]} - e^{-\mathbb{E}[K_2]} + e^{-(\mathbb{E}[K_1] + \mathbb{E}[K_2])}.\end{aligned}\quad (15)$$

The difference is that in (14) we have the term $e^{-\mathbb{E}[K_{1,2}]}$ while, if we assume independence, we have $e^{-(\mathbb{E}[K_1] + \mathbb{E}[K_2])}$ instead. For generalization purposes, considering the rectangles with height model of blocking elements, these expectations are expressed as follows:

$$\begin{cases} \mathbb{E}[K_1] + \mathbb{E}[K_2] &= \int_l \int_w \int_h \int_\theta \lambda_{lwh\theta} (A_{S_{1_{lwh\theta}}} + A_{S_{2_{lwh\theta}}}) \\ \mathbb{E}[K_{1,2}] &= \int_l \int_w \int_h \int_\theta \lambda_{lwh\theta} A_{S_{1_{lwh\theta}} \cup S_{2_{lwh\theta}}}. \end{cases} \quad (16)$$

Therefore, we can see the difference between both expressions: when taking the statistical dependence between the blockings of the 2 links into consideration, it is assumed that both geometric locus may have a region in common, whose area is taken into account just once, contrary to what is done when considering independence between the blockages, when the area of this common region is summed twice. This effect is shown in Fig. 8. This makes that the probability of blockage when we consider correlation of the blockings between the links is higher than in the other case.

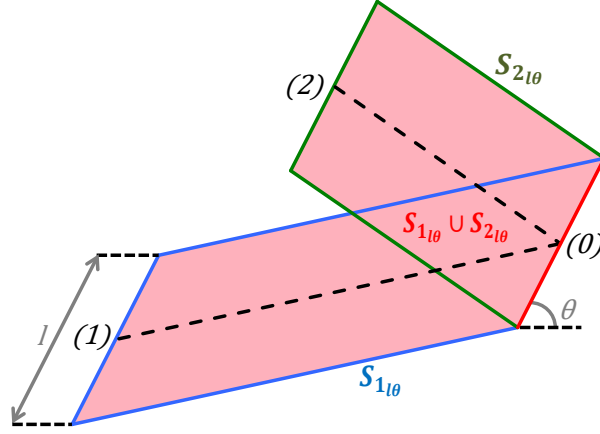


Fig. 8: Geometric locus of links 1 and 2, $S_{1l\theta}$ and $S_{2l\theta}$, respectively, when considering the line segments model of blocking elements with length l and orientation θ .

Finally, if blockages in each link are independent, which happens whenever $A_{S_{1lwh\theta} \cup S_{2lwh\theta}} = A_{S_{1lwh\theta}} + A_{S_{2lwh\theta}} \forall l, w, h, \theta$ (that is, when the blocking regions do not overlap), our expression can also be applied (as stated in [12] as well). When this is not the case, the assumption of independence between the blockings of both links leads to inaccurate results, as will be shown in the simulations section.

B. N Links

In order to generalize the expression above for N links, first we obtain the expression for the case of 3 links. As we have done in the previous section, we are interested in the probability of blockage. Since now we are considering 3 links, we have:

$$\begin{aligned} \mathbb{P}(\text{all}KO) &= 1 - \mathbb{P}(OK_1 \vee OK_2 \vee OK_3) \\ &= 1 - e^{-\mathbb{E}[K_1]} - e^{-\mathbb{E}[K_2]} - e^{-\mathbb{E}[K_3]} + e^{-\mathbb{E}[K_{1,2}]} + e^{-\mathbb{E}[K_{1,3}]} + e^{-\mathbb{E}[K_{2,3}]} - e^{-\mathbb{E}[K_{1,2,3}]}. \end{aligned} \quad (17)$$

At this point, we are ready to generalize the expression for N links [19]:

$$\begin{aligned} \mathbb{P}(\text{all}KO) &= 1 - \mathbb{P}\left(\bigvee_{n=1}^N OK_n\right) \\ &= 1 - \sum_{n=1}^N \mathbb{P}(OK_n) + \sum_{n<m} \mathbb{P}(OK_n \wedge OK_m) \\ &\quad - \sum_{n<m<l} \mathbb{P}(OK_n \wedge OK_m \wedge OK_l) + \dots + (-1)^N \mathbb{P}\left(\bigwedge_{n=1}^N OK_n\right). \end{aligned} \quad (18)$$

In a closed form, this could be written as follows (see [19]):

$$\mathbb{P}(\text{all}KO) = 1 - \mathbb{P}\left(\bigvee_{n=1}^N OK_n\right) = 1 - \sum_{k=1}^N \left((-1)^{k-1} \sum_{\substack{\mathcal{A} \subset \{1, \dots, N\} \\ |\mathcal{A}|=k}} \mathbb{P}\left(\bigwedge_{n \in \mathcal{A}} OK_n\right) \right), \quad (19)$$

where \mathcal{A} with $|\mathcal{A}| = k$ is a subset of $\{1, \dots, N\}$ of k links.

As previously explained, obtaining $\mathbb{P}\left(\bigwedge_{n \in \mathcal{A}} OK_n\right)$ is as simple as considering the area formed by the union of all the blocking regions associated with the links that form the subset \mathcal{A} in each term. In other words:

$$\mathbb{P}\left(\bigwedge_{n \in \mathcal{A}} OK_n\right) = e^{-\mathbb{E}[K_{\mathcal{A}}]}, \quad (20)$$

where $K_{\mathcal{A}}$ is the number of blocking elements that block, at least, one of the links that form the subset \mathcal{A} . This turns the former expression into:

$$\mathbb{P}(\text{all}KO) = 1 - \mathbb{P}\left(\bigvee_{n=1}^N OK_n\right) = 1 - \sum_{k=1}^N \left((-1)^{k-1} \sum_{\substack{\mathcal{A} \subset \{1, \dots, N\} \\ |\mathcal{A}|=k}} e^{-\mathbb{E}[K_{\mathcal{A}}]} \right), \quad (21)$$

with

$$\mathbb{E}[K_{\mathcal{A}}] = \int_l \int_w \int_h \int_{\theta} \lambda_{lwh\theta} A \bigcup_{n \in \mathcal{A}} S_{n_{lwh\theta}}, \quad (22)$$

when assuming the most general model of blocking elements, which are the rectangles with height. The only thing left is to obtain $A \bigcup_{n \in \mathcal{A}} S_{n_{lwh\theta}}$, which is a matter of geometry. It should be highlighted that these results can be applied to any model of blocking elements. For instance, if the line segments model was considered, then the terms to obtain would be $A \bigcup_{n \in \mathcal{A}} S_{n_{l\theta}}$ instead.

IV. APPLICATION TO RELAY-BASED COMMUNICATIONS

In previous sections, we have characterized the effect of blockages in isolated links and in the case of having multiple links, with different models of blocking elements and taking correlation into account. In this section, we are going to use the previous generic results for a concrete application, namely the optimum positioning of a set of relays in a mmWave cell. A set of reference works for relays and can be found in [16], [20], [21], [22], and references therein.

For this purpose, in the first subsection we describe the scenario and consider some issues related to sensitivity and power loss. Finally, we will derive the expression of the probability of blockage (i.e., not being in coverage) in order to minimize it by adjusting the position of the relays.

This section generalizes the previous work [16]. There, a scenario with several nodes located at given non-random concrete positions is considered. In that paper, it is assumed that the blocking elements are circles with a given non-random radius and without height. That work considers that whenever the direct link from the BS to a given node is blocked, it connects to a neighboring node that takes the role of relaying. In our work, we consider blocking elements with random shape and calculate the blocking probability in a cell where there are several relays. This probability of not being in coverage is averaged over the random position of the user, which was not done before and allows to get a global figure a merit in terms of coverage for the whole system and not only for a concrete user position, based on which the position of the relays can then be optimized. Also, our work considers in this section the fact that the receiver has a given sensitivity, which means that transmission will not be possible if the length of the link is too high due to signal attenuation even in a LOS situation. These sensitivity limitations are not considered in [16].

A. Scenario and Problem Definition

We consider a cell of radius R where the BS is placed at the origin, that is $(x_B, y_B) = (0, 0)$. This cell has N relay stations (RSs) indexed by $n = 1, \dots, N$. The goal is to minimize the average probability that a user equipment (UE) does not achieve a successful transmission through any of the available links $\mathbb{P}(\text{all}KO)$ (i.e., is not in coverage), taking power and sensitivity constraints into account. Since we assume that the blockings are uniformly distributed within the considered cell with a certain spatial density, due to the symmetry of the problem, it is deduced that the optimum positions of the relays must be equispaced in azimuth. Therefore, the n_{th} RS is placed at $(x_n, y_n) = (r \cos \psi_n, r \sin \psi_n)$, where $\psi_n = (n-1)\frac{2\pi}{N}$ is its azimuth. The position of a generic UE can be expressed as $(x_U, y_U) = (d \cos \phi, d \sin \phi)$, where ϕ is the azimuth of the UE and d is its distance to the BS. We assume that users are randomly uniformly distributed within the cell as well (which means than ϕ and d are taken from the r.v.'s Φ and D , respectively). An example of the deployment with 3 RSs can be found in Fig. 9.

As far as distances is concerned, we have the following relations:

$$\begin{cases} \|(x_B, y_B) - (x_n, y_n)\| = r \quad \forall n \\ \|(x_n, y_n) - (x_U, y_U)\| = \sqrt{d^2 + r^2 - 2dr \cos(\phi - \psi_n)} \\ \|(x_B, y_B) - (x_U, y_U)\| = d \end{cases} \quad (23)$$

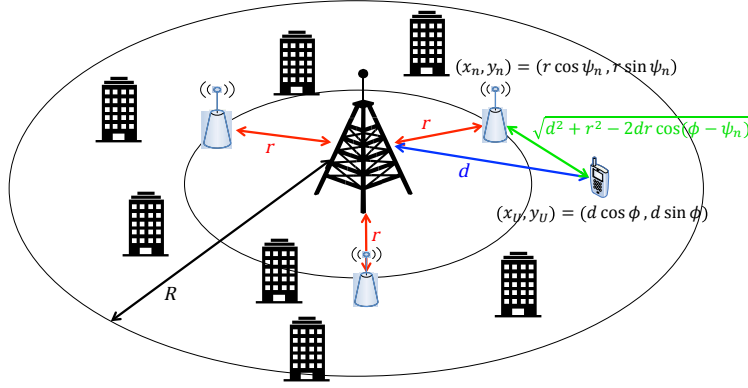


Fig. 9: Example of a deployment with 3 RSs.

The analysis performed in this section focuses on two different types of cells:

- *Sectorized cells*: the cell is divided into N sectors which are served by a single RS each. A UE that is in the n_{th} sector can be connected to just the n_{th} RS or to the BS itself, but not to any other RS.
- *Non-sectorized cells*: each user can be connected to any RS of the cell or to the BS.

For the sake of simplicity, we consider the downlink. In Table I, a set of parameters related to power and propagation are defined. The last 3 parameters, which are the heights, are only used when talking about models of blocking elements that incorporate height.

When considering that the values of the received power must be greater than the sensitivity and taking propagation losses into account, we have a set of constraints that can be formulated through the following indicative functions, in which height is considered: $\mathbb{1}_{S_{BU}}(d)$, $\mathbb{1}_{S_{BR}}(r, h_R)$ and $\mathbb{1}_{S_{R_nU}}(d, \phi, r, h_R)$. S_{BU} , S_{BR} and S_{R_nU} are the sets of points associated to links BU , BR and R_nU , respectively, that fulfill the sensitivity conditions, that is, the received power is greater than the sensitivity values at those points. These additional constraints to the blocking conditions also affect the probability of having successful transmission, that is, being in coverage.

B. Probability of Successful Transmission (Average Coverage Probability)

The objective is to find the optimum position of the relays (i.e., distance r to the BS) and the height of the relays so as to minimize the average probability of not having successful transmission, that is,

$$\min_{r, h_R} \int_0^R \int_{\phi_s}^{\phi_e} \mathbb{P}(\text{all } KO | D = d, \Phi = \phi) f_D(d) f_\Phi(\phi) d d d \phi, \quad (24)$$

Concept	Description
P_{T_B}	BS transmission power
P_{T_R}	RS transmission power
P_{R_R}	RS reception power
P_{R_U}	UE reception power
S_R	RS sensitivity
S_U	UE sensitivity
G_B	BS gain
G_R	RS gain
G_U	UE gain
k	Path-loss at reference distance
α	Path-loss exponent
H_B	BS height
h_R	RS height
H_U	UE height

TABLE I: Sensitivity parameters.

where $f_D(d)$ and $f_\Phi(\phi)$ are the pdf's of the distance and azimuth of a user located at a random position, which is detailed in what follows.

Note that this is the general expression and can have many versions. For instance, if we consider the line segments or the rectangles models of blocking elements, then heights will not be taken into account and h_R will not appear in the expressions.

On the other hand, the limits of the integral with respect to the azimuth ϕ and the pdf $f_\Phi(\phi)$ depend on whether the cell is sectorized or not, as explained above. Consequently, we focus only on the term $\mathbb{P}(\text{all } KO | D = d, \Phi = \phi)$. Additionally, from now on, and for the sake of simplicity, we omit to write $|D = d, \Phi = \phi$, but it should not be forgotten that the expressions that follow are just for a specific position of the UE and the RS.

1) Sectorized Cells: As explained above, in sectorized cells, cells are divided into N different sectors and the UE can be only connected to the RS of the sector where it is located or directly to the BS (see Fig. 10).

A UE is considered to be within the n_{th} sector whenever its azimuth is between $\psi_{n_s} = \psi_n - \frac{\pi}{N}$ and $\psi_{n_e} = \psi_n + \frac{\pi}{N}$, which are the angles that limit that region. With this in mind, in this case,

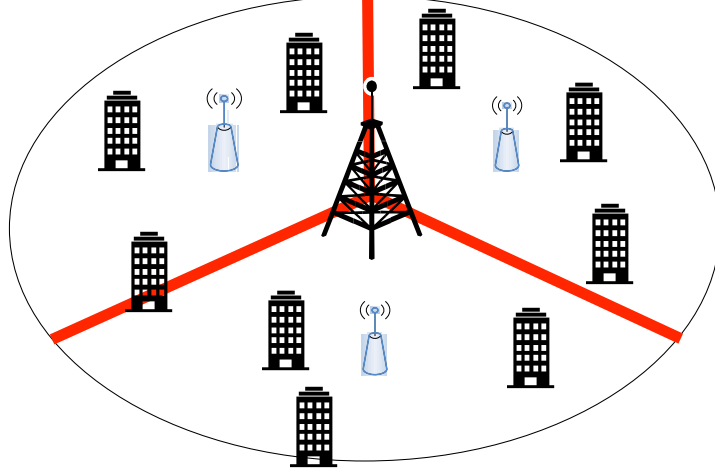


Fig. 10: Example of a deployment with 3 RSs in a sectorized cell.

the random position of a user in the n_{th} sector can be characterized by the following pdf's²:

$$\begin{cases} f_D(d) = \frac{2d}{R^2} & \text{where } 0 \leq d \leq R \\ f_\Phi(\phi) = \frac{N}{2\pi} & \text{where } \psi_{n_s} \leq \phi \leq \psi_{n_e}. \end{cases} \quad (25)$$

By applying (21) and (22) to sectorized cells, we have that the probability of not having successful transmission is:

$$\begin{aligned} \mathbb{P}(\text{all}KO) &= 1 - \mathbb{P}(OK_{BU}) - \mathbb{P}(OK_{BR_n} \wedge OK_{R_nU}) + \mathbb{P}(OK_{BU} \wedge OK_{BR_n} \wedge OK_{R_nU}) \\ &= 1 - e^{-\mathbb{E}[K_{BU}]} \mathbb{1}_{S_{BU}}(d) - e^{-\mathbb{E}[K_{BR_n, R_nU}]} \mathbb{1}_{S_{BR}}(r, h_R) \mathbb{1}_{S_{R_nU}}(d, \phi, r, h_R) \\ &\quad + e^{-\mathbb{E}[K_{BU, BR_n, R_nU}]} \mathbb{1}_{S_{BU}}(d) \mathbb{1}_{S_{BR}}(r, h_R) \mathbb{1}_{S_{R_nU}}(d, \phi, r, h_R). \end{aligned} \quad (26)$$

The only thing left is to calculate the area of the union of such blocking regions for every possible length, width, height and orientation of the blocking elements if, for instance, the rectangles with height model, which is the most general, is considered. In order to give an idea, Fig. 11 shows three parallelograms that belong to the BU , BR_n and R_nU links when having the line segments model of blocking elements with a certain length l and orientation θ .

² Since we assume users to be uniformly distributed within the cell, a division of areas gives us that $Pr(D \leq d) = \frac{\pi d^2}{\pi R^2} = \frac{d^2}{R^2}$. Therefore, we obtain, through derivation, $f_D(d) = \frac{2d}{R^2}$. This pdf applies to both sectorized and non-sectorized cells.

On the other hand, $f_\Phi(\phi)$ is a uniform pdf that changes depending on whether the user is located, that is, if the cell is sectorized or not.

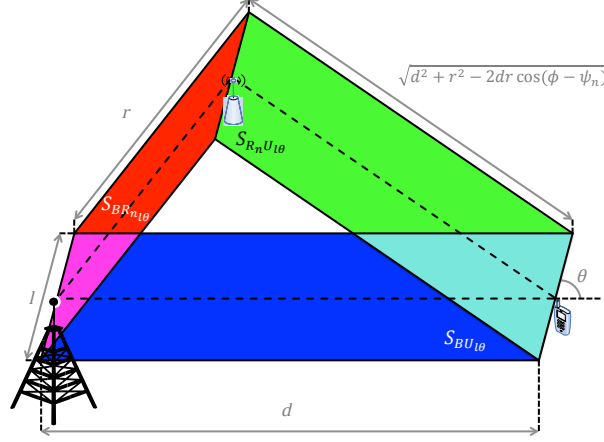


Fig. 11: Parallelograms of the three links in a sectorized cell, with line segments as blocking elements with length l and orientation θ .

In some practical cases, relays may be placed in a way such that no blockings between them and the BS will happen. In other words, the BR_n link will be in LOS, that is $K_{BR_n} = 0$. This makes that $K_{BR_n lwh\theta} = 0 \forall l, w, h, \theta$, which means that no centers of blockage fall within $S_{BR_n lwh\theta}$ and, therefore, neither in $S_{BR_n lwh\theta} \cap S_{R_n U lwh\theta}$ nor in $S_{BR_n lwh\theta} \cap S_{BU lwh\theta}$. Consequently,

$$\begin{aligned}
 \mathbb{P}(\text{all}KO) &= 1 - \mathbb{P}(OK_{BU}) - \mathbb{P}(OK_{BR_n} \wedge OK_{R_n U}) + \mathbb{P}(OK_{BU} \wedge OK_{BR_n} \wedge OK_{R_n U}) \\
 &= 1 - e^{-\mathbb{E}[K_{BU}|K_{BR_n}=0]} \mathbb{1}_{S_{BU}}(d) \\
 &\quad - e^{-\mathbb{E}[K_{R_n U}|K_{BR_n}=0]} \mathbb{1}_{S_{BR}}(r, h_R) \mathbb{1}_{S_{R_n U}}(d, \phi, r, h_R) \\
 &\quad + e^{-\mathbb{E}[K_{BU, R_n U}|K_{BR_n}=0]} \mathbb{1}_{S_{BU}}(d) \mathbb{1}_{S_{BR}}(r, h_R) \mathbb{1}_{S_{R_n U}}(d, \phi, r, h_R), \tag{27}
 \end{aligned}$$

where

$$\begin{cases}
 \mathbb{E}[K_{BU}|K_{BR_n}=0] = \int_l \int_w \int_h \int_\theta \lambda_{lwh\theta} A_{S_{BU lwh\theta} \setminus S_{BR_n lwh\theta}} \\
 \mathbb{E}[K_{R_n U}|K_{BR_n}=0] = \int_l \int_w \int_h \int_\theta \lambda_{lwh\theta} A_{S_{R_n U lwh\theta} \setminus S_{BR_n lwh\theta}} \\
 \mathbb{E}[K_{BU, R_n U}|K_{BR_n}=0] = \int_l \int_w \int_h \int_\theta \lambda_{lwh\theta} A_{(S_{BU lwh\theta} \cup S_{R_n U lwh\theta}) \setminus S_{BR_n lwh\theta}}.
 \end{cases} \tag{28}$$

2) *Non-Sectorized Cells*: If the cell is not sectorized, that is, if a user can be connected to any RS in the cell, the position of the user follows the following distributions²:

$$\begin{cases}
 f_D(d) = \frac{2d}{R^2} \quad \text{where } 0 \leq d \leq R \\
 f_\Phi(\phi) = \frac{1}{2\pi} \quad \text{where } 0 \leq \phi \leq 2\pi.
 \end{cases} \tag{29}$$

Gathering everything together, the formulation of not having a successful transmission (i.e., not being in coverage) in the not sectorized case with N relays is (in the following expressions, $n = N + 1$ refers to the direct link between the BS and the UE):

$$\begin{aligned} \mathbb{P}(\text{all}KO) &= 1 - \mathbb{P}\left(\bigvee_{n=1}^{N+1} OK_n\right) = 1 - \sum_{k=1}^{N+1} \left((-1)^{k-1} \sum_{\substack{\mathcal{A} \subset \{1, \dots, N+1\} \\ |\mathcal{A}|=k}} \mathbb{P}\left(\bigwedge_{n \in \mathcal{A}} OK_n\right) \right) \\ &= 1 - \sum_{k=1}^{N+1} \left((-1)^{k-1} \sum_{\substack{\mathcal{A} \subset \{1, \dots, N+1\} \\ |\mathcal{A}|=k}} \left(e^{-\mathbb{E}[K_{\mathcal{A}}]} \prod_{n \in \mathcal{A}} \mathbb{1}_{S_n}(d, \phi, r, h_R) \right) \right), \end{aligned}$$

with

$$\mathbb{1}_{S_n}(d, \phi, r, h_R) = \begin{cases} \mathbb{1}_{S_{BR}}(r, h_R) \mathbb{1}_{S_{R_n U}}(d, \phi, r, h_R) & \text{if } n \leq N \\ \mathbb{1}_{S_{BU}}(d) & \text{if } n = N + 1. \end{cases} \quad (30)$$

If we consider the rectangle based model with height, we have:

$$\mathbb{E}[K_{\mathcal{A}}] = \int_l \int_w \int_h \int_{\theta} \mathbb{E}[K_{\mathcal{A}_{lwh\theta}}] = \int_l \int_w \int_h \int_{\theta} \lambda_{lwh\theta} A \cup_{n \in \mathcal{A}} S_{n_{lwh\theta}}, \quad (31)$$

where $\lambda_{lwh\theta} = \lambda f_L(l) dl f_W(w) dw f_H(h) dh f_{\Theta}(\theta) d\theta$ and

$$S_{n_{lwh\theta}} = \begin{cases} S_{BR_{n_{lwh\theta}}} \cup S_{R_n U_{lwh\theta}} & \text{if } n \leq N \\ S_{BU_{lwh\theta}} & \text{if } n = N + 1. \end{cases} \quad (32)$$

The assumption that all the BR links are in LOS, that is, there are no blockages between the BS and the RS, can also be made here, which implies that

$$S_{n_{lwh\theta}} = \begin{cases} S_{R_n U_{lwh\theta}} \setminus \left(\bigcup_{m \in \mathcal{B}} S_{BR_{m_{lwh\theta}}} \right) & \text{if } n \leq N \\ S_{BU_{lwh\theta}} \setminus \left(\bigcup_{m \in \mathcal{B}} S_{BR_{m_{lwh\theta}}} \right) & \text{if } n = N + 1, \end{cases} \quad (33)$$

where $\mathcal{B} = \{1, \dots, N\}$.

V. RESULTS

In order to validate the analytic expressions derived in this work, we will compare them with some Monte Carlo numerical simulations in which blockages are thrown randomly within a cell following a uniform spatial PPP distribution. The model of blocking elements considered is the one of rectangles with height.

Parameter	Description	Value
R	Cell radius	300 m
H_B	BS height	40 m
H_U	UE height	1.5 m

TABLE II: Parameters taken in the simulations for the single-link cases.

A. Single-Link

In this subsection we consider a single link (i.e., no relays are deployed) without taking into account sensitivity. The parameters considered in this simulation are detailed in Table II.

First, we obtain the probability that a UE at a given distance d from the BS (which is at the center of the cell) is blocked. This distance is evaluated from 0 to the radius R of the cell. Following the expressions for the blockage probability in (3) and the one of the mean value of the number of blockages with the rectangles with height model in (10), we derive the formula to obtain the blockage probability analytically. In Fig. 12, we take blocking elements with their lengths, widths, heights and orientations following uniform distributions, that is:

$$\left\{ \begin{array}{l} L \sim \mathcal{U}[0, L_{max}] \quad \text{with} \quad L_{max} = 30 \text{ m} \\ W \sim \mathcal{U}[0, W_{max}] \quad \text{with} \quad W_{max} = 30 \text{ m} \\ H \sim \mathcal{U}[0, H_{max}] \quad \text{with} \quad H_{max} = 30 \text{ m} \\ \Theta \sim \mathcal{U}[0, \Theta_{max}] \quad \text{with} \quad \Theta_{max} = \pi \text{ rad} \end{array} \right. \quad (34)$$

Then, we analyze the blockage probability for the cases where the density of blockages λ is $1 \cdot 10^{-4} \text{ m}^{-2}$ and $2.2 \cdot 10^{-4} \text{ m}^{-2}$.

We can clearly see that the simulation results perfectly match the analytical results. The relation between the blockage probability, $P(KO)$, and the distance d to the BS is almost linear and, as expected, the denser the buildings are and the further from the BS the users are located, the more likely the UEs are blocked.

Next, we want to see in detail the influence of the density of blockages on the overall blockage probability of the users that are within the cell. To obtain the expression of the mean blockage probability of all the cell, we take into account again expressions (3) and (10), which have served us to obtain the blockage probability on a given position. In this case we should take the mean

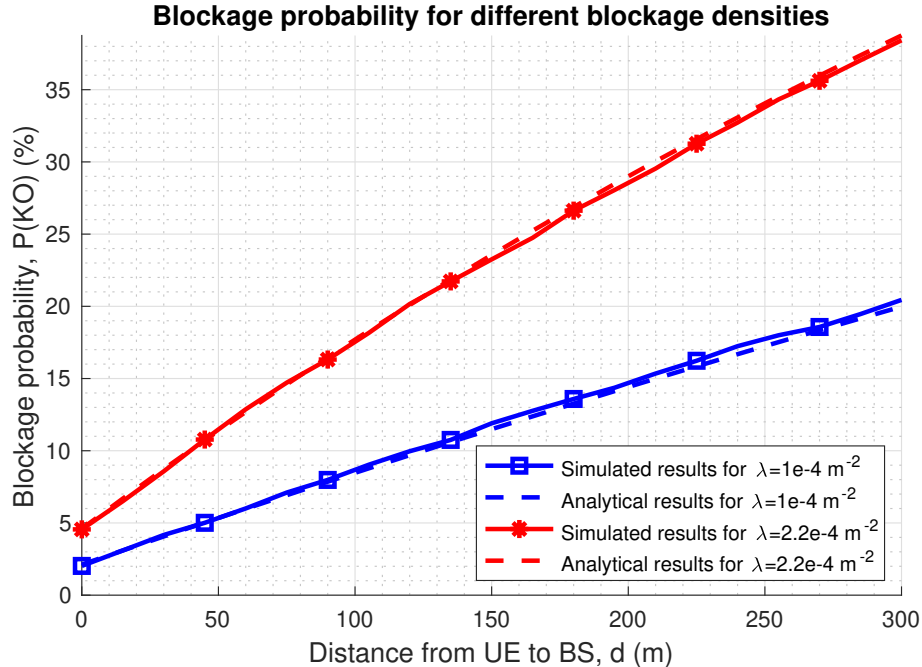


Fig. 12: Blockage probability vs distance from the BS depending on the blockage density.

value by considering that users are distributed uniformly throughout the cell following the same distributions that we had in (29). Then, the mean analytic probability of blockage is:

$$\begin{aligned}
 \overline{P(KO)} &= \int_0^{2\pi} \int_0^R P(KO|D=d, \Phi=\phi) f_D(d) f_\Phi(\phi) d d d \phi \\
 &= \int_0^{2\pi} \int_0^R (1 - e^{-(\eta_{BU}\beta d + \mu_{BU}p)}) d \frac{2}{R^2} \frac{1}{2\pi} d d d \phi \\
 &= 1 + \frac{2(\eta_{BU}\beta R - e^{\eta_{BU}\beta R} + 1)}{(\eta_{BU}\beta R)^2} e^{-(\eta_{BU}\beta R + \mu_{BU}p)}, \tag{35}
 \end{aligned}$$

where η_{BU} and μ_{BU} are the η and μ parameters particularized for the BU link. The previous expression in closed-form can also be considered a contribution of this work. In Fig. 13, the values of all the parameters are the same as before except the maximum height H_{max} of the blocking elements. Now, in addition to the height of 30 m considered before, we also considered 40 m to gain more insights into the scenario. In Fig. 13 we can see the results, from which it can be concluded, as expected, that the higher and denser the buildings are, the more likely the users are going to be blocked.

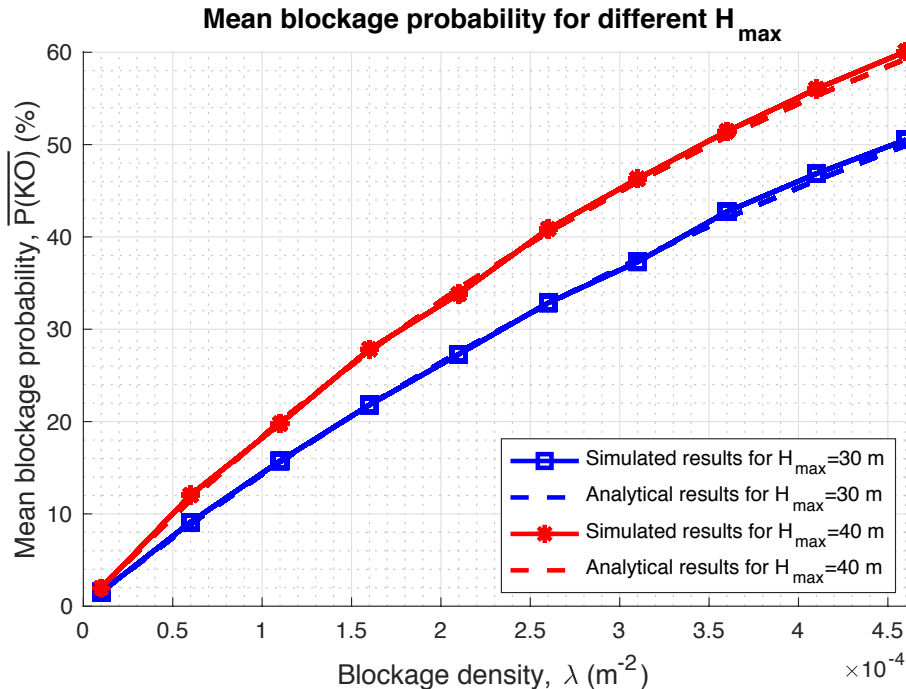


Fig. 13: Overall average blockage probability depending on the blockage density and the maximum height of the buildings.

B. Relay Deployment

This subsection validates and analyzes the results for the case in which 3 RSs are deployed within the cell. Here we consider the sectorized case, that is, the user can only be connected to the BS directly or via the RS of the sector where it is located.

In the first case, shown in Fig. 14, we are interested in comparing the simulation with the analytic results. Relays are placed at a distance of $r = 180$ m from the BS and at a height of $h_R = 20$ m. Both the length L and width W of the blockages are set to 15 m, while the height and orientation again follow a uniform distribution such that $H \sim \mathcal{U}[0, H_{\max}]$ with $H_{\max} = 30$ m and $\Theta \sim \mathcal{U}[0, \Theta_{\max}]$ with $\Theta_{\max} = \pi$ rad respectively. Then, as we had in the single-link situation of Fig. 12, we evaluate the probability of blockage that a user experiences at a given distance from the BS. Since we are placing RSs, it is important to take into account the azimuth at which the user is located, since we will obtain different results depending on whether the user is close or not, from an azimuth point of view, to the RS of the corresponding sector.

Specifically, we assume that the first of the 3 RSs is placed at $\psi_n = 0^\circ$, whose sector lays between $\psi_{n_s} = -60^\circ$ and $\psi_{n_e} = 60^\circ$. We only focus on this first sector and obtain the blockage

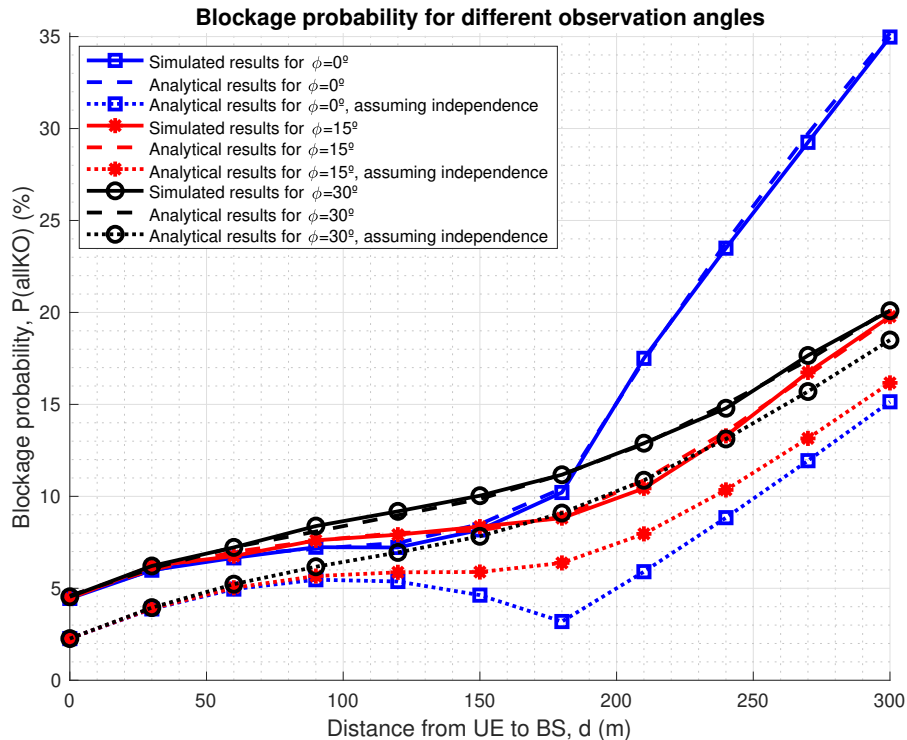


Fig. 14: Blockage probability at a given distance from the BS depending on the azimuth of observation.

probability at a given distance d from the BS for three different azimuths for the user at $\phi = 0^\circ$, $\phi = 15^\circ$ and $\phi = 30^\circ$. For each angle we show the simulated results, the analytical results, and the analytical results assuming independence among the blocking elements of each link.

- *UE at $\phi = 0^\circ$ (blue lines with square markers)*: in this situation, the azimuths of the user and the RS are the same. We can see that if the user is located at a distance greater than 180 m from the center, there is a sharp increase on the blockage probability. This is due to the fact that in this case we are not exploiting the diversity gain among the blocking elements of the different links. In other words: if the link between the BS and the RS is blocked, the communication between via the RS will not be possible. Furthermore, since the the UE's height is smaller than the RS's height, the BU link will be blocked as well. Consequently, the three links are highly correlated. Regarding the assumption that the blocking elements are independent in each link, we can see that the result is completely different, leading us to much more optimistic results. As commented, if the BR link is blocked, the BU link

will be blocked, too. However, the independence assumption considers that this may not be always the case, which is not realistic. This is the reason why the independence assumption produces lower blockage probabilities.

- *UE at $\phi = 15^\circ$ (red lines with asterisc markers)*: in this case, by moving azimuthally 15° aside from ψ_n , we see that the results are much better than in the previous case. This is for the same reason as discussed before: in this situation, if the BR link is blocked, the BU link may not be blocked, and viceversa. Here we are exploiting the diversity of blockages and we do not find the previous sharp increase in the blockage probability for $d = 180$ m.
- *UE at $\phi = 30^\circ$ (black lines with circle markers)*: in this last situation, the blockage probability from $d = 180$ m is lower than in the first one of $\phi = 0^\circ$ because, again, it exploits the diversity gain among the blocking elements in the different links, but it is not lower than in the case of $\phi = 15^\circ$. This is for an obvious reason: even though we have the effect of this diversity gain, at $\phi = 30^\circ$ the UE is further from the RS than in the $\phi = 15^\circ$ case, which makes more likely to have more blocking elements in the RU link and, therefore, the blockage probability increases.

As a conclusion, we clearly see that there is a trade-off between exploiting the diversity gain of the blocking elements among the different links and not being located very far from the RS so as to reduce the probability of being blocked in the RU link. This aspect should be taken into account in the relay deployment. To investigate that trade-off, we want to obtain the positions of the RSs that minimize the overall probability of blockage of the users within the cell, that is, the average probability of not being in coverage. Therefore, in Fig. 15 we plot the blockage probability depending on the distance r between the BS and the RS and its height h_R . Moreover, to get a first approximation of what the results in a real deployment could look like, we have included the maximum power constraints and sensitivity parameters, summarized in Table III. In this case, we consider that the blocking elements are defined with the same distributions as we had in (34). We also include the blockage probability when RSs are not deployed, obtained from (35).

Some important conclusions that the figure raises is that the position of the RSs where $\overline{P(\text{all}KO)}$ is minimum is not at half of the radius of the cell (that would be at 150 m in this case) but somehow closer to the edges of the cell, which is consistent with the results shown in Fig. 14. Moreover, it should be highlighted that considering sensitivity and power constraints, which is a novel contribution to this topic, has a high impact on the performance and deployment.

Parameter	Description	Value
P_{T_B}	BS transmission power	-5 dBm
P_{T_R}	RS transmission power	-10 dBm
S_R	RS sensitivity	-95 dBm
S_U	UE sensitivity	-95 dBm
G_B	BS gain	10.6 dB
G_R	RS gain	5 dB
G_U	UE gain	-1 dB
k	Path-loss at reference distance	1.35
α	Path-loss exponent	4

TABLE III: Parameters taken for the evaluation of the positioning of the relays.

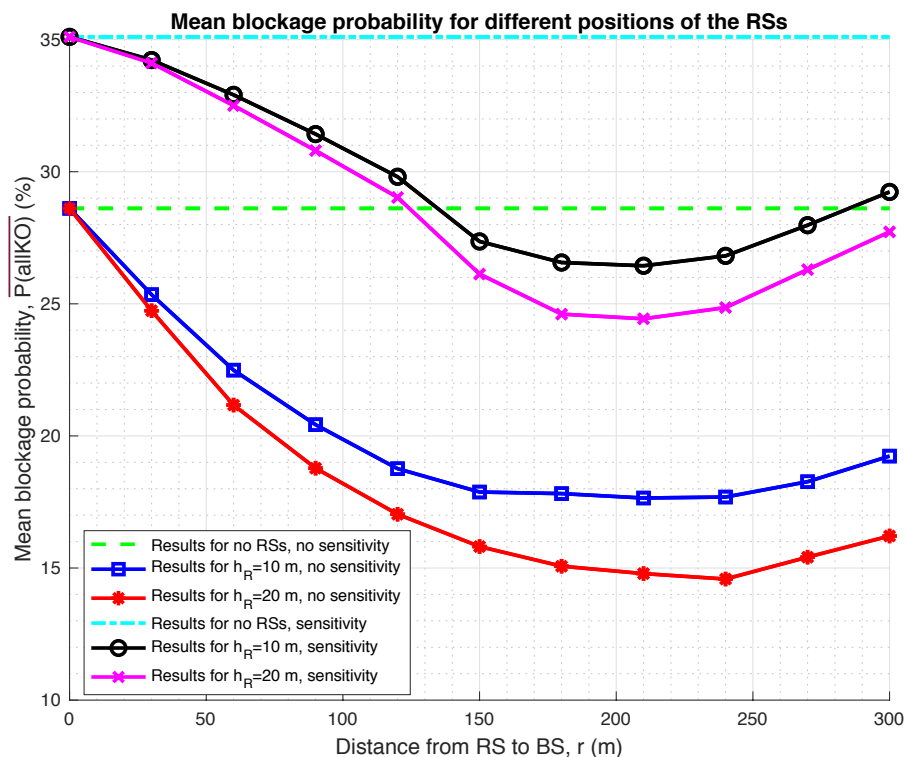


Fig. 15: Overall blockage probability depending on the position of the RSs.

Firstly, it is shown that, when including the sensitivity in the analysis, the blockage probability increases by more than 5%. Secondly, the distance r from the BS to the RS where the minimum of blockage probability is achieved is slightly reduced when compared to the situation in which sensitivity and power constraints are not taken into account.

VI. SUMMARY AND CONCLUSIONS

In this paper, we have derived the blockage model in which the base of the blocking element is a rectangle and it has a finite height. This is something to be remarked, since it is the model that fits best actual buildings in urban environments.

Moreover, we have been able to generalize the expression of the probability of blockage for N different links to any model of blocking elements while taking into account the statistical dependence of the blocking elements of each link and considering the rectangles with height model of blocking elements. As we have checked through different analytic expressions and simulations, the effect of correlation is not negligible and must be taken into account in the cell deployment.

Finally, the obtained expressions have been applied to our scenario where relays are deployed within the cell in order to evaluate which is the position of the relays for which the average probability of blockage is minimized, that is, to maximize the overall coverage. Furthermore, maximum power constraints and sensitivity parameters have been considered so as to have a better approach to the real scenario that such cellular deployments should face.

As next steps, it could be interesting to analyze both analytically and with field testing a real scenario and make a comparison between them so as to check how the derived expressions fit the real world. Also, the analysis of the effect of the mobility of the users and its impact on the duration of the blockage events is left for future work.

ACKNOWLEDGMENT

The work presented in the present paper has been funded through the grant 2017 SGR 578 (funded by the Catalan Government—Secretaria d'Universitats i Recerca, Departament d'Empresa i Coneixement, Generalitat de Catalunya, AGAUR) and the project TEC2016-77148-C2-1-R (AEI/FEDER, UE): 5G&B-RUNNER-UPC (funded by the Agencia Estatal de Investigación, AEI, and Fondo Europeo de Desarrollo Regional, FEDER).

REFERENCES

- [1] J. G. Andrews, T. Bai, M. N. Kulkarni, A. Alkhateeb, A. K. Gupta, and R. W. Heath, "Modeling and analyzing millimeter wave cellular systems," *IEEE Trans. on Communications*, vol. 65, no. 1, pp. 403–430, Jan. 2017.
- [2] E. Dahlman, S. Parkvall, and J. Sköld, *5G NR: The Next Generation Wireless Access Technology*. London (UK): Academic Press, 2018.

- [3] T. S. Rappaport, R. W. Heath, R. C. Daniels, and J. N. Murdock, *Millimeter Wave Wireless Communications*. Massachusetts (USA): Prentice Hall, 2015.
- [4] R. W. Heath, N. González-Prelcic, S. Rangan, W. Roh, and A. M. Sayeed, “An overview of signal processing techniques for millimeter wave MIMO systems,” *IEEE Journal on Selected Areas in Signal Processing*, vol. 10, no. 3, pp. 436–453, Apr. 2016.
- [5] T. Bai, R. Vaze, and R. W. Heath, “Using random shape theory to model blockage in random cellular networks,” in *IEEE International Conference on Signal Processing and Communications (SPCOM)*, Bangalore (India), July 2012, pp. 1–5.
- [6] —, “Analysis of blockage effects on urban cellular networks,” *IEEE Trans. on Wireless Communications*, vol. 13, no. 9, pp. 5070–5083, Sep. 2014.
- [7] D. Stoyan, W. Kendall, and J. Mecke, *Stochastic Geometry and Its Applications*, 2nd ed. Hoboken, NJ, USA: Wiley, 1995.
- [8] F. Baccelli and B. Błaszczyszyn, *Stochastic Geometry and Wireless Networks, Volume I - Theory*. Delft, The Netherlands: NOW, 2009.
- [9] M. Haenggi, *Stochastic Geometry for Wireless Networks*. Cambridge: Cambridge University Press, 2013.
- [10] R. Cowan. (1989) Objects arranged randomly in space: An accessible theory. In *Advances in Applied Probability*. [Online]. Available: <http://www.jstor.org/stable/1427635>
- [11] A. K. Gupta, J. G. Andrews, and R. W. Heath, “Macrodiversity in cellular networks with random blockages,” *IEEE Trans. on Wireless Communications*, vol. 17, no. 2, pp. 996–1010, Feb. 2018.
- [12] —, “Impact of correlation between link blockages on macro-diversity gains in mmwave networks,” in *IEEE International Conference on Communications Workshops (ICC Workshops)*, Kansas City, MO (USA), May 2018, pp. 1–6.
- [13] E. Hriba and M. Valenti, “Correlated blocking in mmWave cellular networks: Macrodiversity, outage, and interference,” *Electronics*, vol. 8, no. 1187, pp. 1–17, Oct. 2019.
- [14] Y. Liu, Y. Jian, R. Sivakumar, and D. Blough, “Optimal access point placement for multi-AP mmWave WLANs,” in *ACM International Conference on Modeling, Analysis and Simulation of Wireless and Mobile Systems (MSWiM)*, Miami Beach (USA), Nov. 2019, pp. 35–44.
- [15] K. Belbase, Z. Zhang, H. Jiang, and C. Tellambura, “Coverage analysis of millimeter wave decode-and-forward networks with best relay selection,” *IEEE Access*, vol. 6, pp. 22 670–22 683, Apr. 2018.
- [16] S. Kwon and J. Widmer, “Relay selection for mmWave communications,” in *IEEE International Symposium on Personal, Indoor, and Mobile Radio Communications (PIMRC)*, Montreal (Canada), Oct. 2017, pp. 1–6.
- [17] R. W. Heath, M. Kountouris, and T. Bai, “Modeling heterogeneous network interference using Poisson point processes,” *IEEE Trans on Signal Processing*, vol. 61, no. 16, pp. 4114–4126, Aug. 2013.
- [18] A. Papoulis and S. U. Pillai, *Probability, Random Variables and Stochastic Processes*. New York: McGraw-Hill Higher Education, 2002.
- [19] G. Modica and L. Pogliolini, *A First Course in Probability and Markov Chains*. Wiley, 2012.
- [20] N. Wei, X. Lin, and Z. Zhang, “Optimal relay probing in millimeter-wave cellular systems with device-to-device relaying,” *IEEE Transactions on Vehicular Technology*, vol. 65, no. 12, pp. 10 218–10 222, Dec. 2016.
- [21] Y. Yan, Q. Hu, and D. M. Blough, “Path selection with amplify and forward relays in mmwave backhaul networks,” in *IEEE 29th Annual International Symposium on Personal, Indoor and Mobile Radio Communications (PIMRC)*, Bologna, Italy, Sept. 2018.
- [22] Q. Hu and D. M. Blough, “Relay selection and scheduling for millimeter wave backhaul in urban environments,” in *2017 IEEE 14th International Conference on Mobile Ad Hoc and Sensor Systems (MASS)*, Orlando, FL (USA), Oct. 2017.